

# Dihapto-Coordinated Amide, Ester, and Aldehyde Complexes and Their Role in Decarbonylation

Peter M. Graham, Christopher J. Mocella, Michal Sabat, and W. Dean Harman\*

Department of Chemistry, University of Virginia, PO Box 400319,  
Charlottesville, Virginia 22904-4319

Received December 10, 2004

The  $\pi$ -basic metal fragment  $\{\text{TpW}(\text{NO})(\text{PMe}_3)\}$  forms thermally stable  $\eta^2$  complexes with acetaldehyde, acetone, ethyl acetate, methyl formate, and *N,N*-dimethylformamide (where Tp = hydridotris(pyrazolyl)borate). The related system  $\{\text{TpMo}(\text{NO})(\text{MeIm})\}$  (MeIm = 1-methylimidazole) also forms stable  $\eta^2$  complexes with acetone, methyl formate, and *N,N*-dimethylformamide. When the tungsten fragment is combined with a carboxylic acid, oxidative addition yields a seven-coordinate hydride complex. These results are compared to those observed for analogous Re and Os systems.  $\text{TpMo}(\text{NO})(\text{MeIm})(\eta^2\text{-DMF})$  and  $\text{TpW}(\text{NO})(\text{PMe}_3)(\eta^2\text{-DMF})$  are rare examples of  $\eta^2$  amide complexes, demonstrating the exceptional strength of these group 6  $\pi$  bases.

## Introduction

Transition metals that interact with aldehydes, ketones, and carboxylic acid derivatives have been extensively explored in the context of synthetic chemistry. Typically these metals act as Lewis acids, enhancing the electrophilic nature of the carbonyl through oxygen coordination (i.e.,  $\eta^1$ ).<sup>1</sup> Examples include the catalysis of nucleophilic substitution, conjugate addition,<sup>2,3</sup> and cycloaddition reactions.<sup>4</sup> In some cases, the metal and associated ligands are able to influence the stereochemistry in these reactions.<sup>5,6</sup> In contrast, complexes in which the metal coordinates the carbonyl through both the carbon and the oxygen are far less common (herein, the term ‘carbonyl’ refers only to compounds of the form RCOR’, not to M-CO). While a number of  $\eta^2$ -aldehyde and ketone complexes are known,<sup>7–11</sup> only three reports of isolable  $\eta^2$  ester or amide complexes have appeared in the literature to date.<sup>12–14</sup> Dihapto coordination of the CO group drastically *reduces* the electrophilic nature of the carbonyl and minimizes its interaction with the neighboring heteroatom.

The higher energy LUMO in esters and amides makes them poor  $\pi$  acids; thus, forming a stable  $\pi$  complex requires an extremely  $\pi$ -basic metal fragment.<sup>12,14</sup> While pentaammineosmium(II) is a powerful  $\pi$  base and readily forms robust  $\pi$  complexes with aldehydes and ketones,<sup>15,16</sup> ester and amide complexes with this metal are far too labile to be isolated.<sup>17</sup> The stronger  $\pi$  bases  $\{\text{TpRe}(\text{CO})(\text{MeIm})\}$ ,  $\{\text{TpMo}(\text{NO})(\text{MeIm})\}$ , and  $\{\text{TpW}(\text{NO})(\text{PMe}_3)\}$ , first developed in the context of arene activation,<sup>14,18,19</sup> provide an opportunity to explore the properties of  $\pi$ -bound carbonyl complexes for a broad range of carbonyls and metals. Rhenium complexes of esters, imides, anhydrides, and the pseudo-amide *N*-acetylpyrrole were first reported in 2002.<sup>13</sup> Since their disclosure, however, the group 6 analogues  $\{\text{TpW}(\text{NO})(\text{PMe}_3)\}$  and  $\{\text{TpMo}(\text{NO})(\text{MeIm})\}$  have been developed, which, in addition to other carbonyls, bind the parent amide, *N,N*-dimethylformamide (DMF). Thus, we felt that a more comprehensive exploration of these group 6 systems in comparison to their group 7 and 8 counterparts would be instructive.

## Results

Tungsten complexes of the form  $\text{TpW}(\text{NO})(\text{PMe}_3)(\eta^2\text{-RC}(\text{O})\text{X})$  were prepared by stirring the complex  $\text{TpW}(\text{NO})(\text{PMe}_3)(\eta^2\text{-benzene})$  in a solution of the desired ligand  $\text{RC}(\text{O})\text{X}$ , where R = CH<sub>3</sub> or H; X = OR, NR<sub>2</sub>, CH<sub>3</sub>). Molybdenum complexes were prepared by reduction of the Mo(I) precursor  $\text{TpMo}(\text{NO})(\text{MeIm})\text{Br}$  in the presence of the desired ligand  $\text{R}(\text{CO})\text{X}$ . Infrared and electrochemical data for these carbonyl complexes are summarized in Table 1.

\* To whom correspondence should be addressed. E-mail: wd5z@virginia.edu.

(1) Shambayati, S.; Crow, W. E.; Schreiber, S. L. *Angew. Chem., Int. Ed. Engl.* **1990**, *29*, 256.

(2) Yus, M.; Pastor, I. M.; Gomis, J. *Tetrahedron* **2001**, *57*, 5799.

(3) Evans, D. A.; Willis, M. C.; Johnston, J. N. *Org. Lett.* **1999**, *1*, 865–868.

(4) Andres, C.; Garcia-Valverde, M.; Nieto, J.; Pedrosa, R. *J. Org. Chem.* **1999**, *64*, 5230–5236.

(5) Kagan, H. B.; Riant, O. *Chem. Rev.* **1992**, *92*, 1007–1019.

(6) Narasaka, K. *Synthesis* **1991**, 1–11.

(7) Mingos, D. M. P. *Comprehensive Organometallic Chemistry*; Pergamon: Oxford, 1982; Vol. 3.

(8) Shambayati, S.; Schreiber, S. L. *Comprehensive Organic Synthesis*; Pergamon: New York, 1991; Vol. 1.

(9) Huang, Y. H.; Gladysz, J. A. *J. Chem. Educ.* **1988**, *65*, 298–303.

(10) Schuster, D. M.; White, P. S.; Templeton, J. L. *Organometallics* **2000**, *19*, 1540–1548.

(11) Gladysz, J. A.; Boone, B. *J. Angew. Chem., Int. Ed. Engl.* **1997**, *36*, 550–583.

(12) Burkey, D. J.; Debad, J. D.; Legzdins, P. *J. Am. Chem. Soc.* **1997**, *119*, 1139–1140.

(13) Meiere, S. H.; Ding, F.; Friedman, L.; Sabat, M.; Harman, W. D. *J. Am. Chem. Soc.* **2002**, *124*, 13506–13512.

(14) Graham, P.; Meiere, S. H.; Sabat, M.; Harman, W. D. *Organometallics* **2003**, *22*, 4364–4366.

(15) Harman, W. D.; Fairlie, D. P.; Taube, H. *J. Am. Chem. Soc.* **1986**, *108*, 8223–8227.

(16) Harman, W. D.; Sekine, M.; Taube, H. *J. Am. Chem. Soc.* **1988**, *110*, 2439–2445.

(17) Harman, W. D. In *Chemistry*; Ph.D. dissertation, Stanford University, 1987.

(18) Meiere, S. H.; Keane, J. M.; Gunnoe, T. B.; Sabat, M.; Harman, W. D. *J. Am. Chem. Soc.* **2003**, *125*, 2024–2025.

(19) Mocella, C. J.; Delafuente, D. A.; Keane, J. M.; Warner, G. R.; Friedman, L. A.; Sabat, M.; Harman, W. D. *Organometallics* **2004**, *23*, 3772–3777.

**Table 1. Infrared and Cyclic Voltammetric Data for TpW(NO)(PMe<sub>3</sub>)(L) and TpMo(NO)(MeIm)(L)**

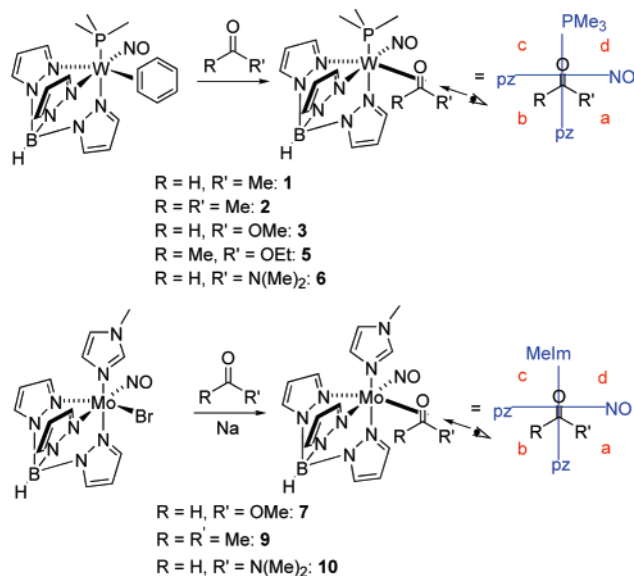
Complex	Metal	Ligand (L)	$\nu_{\text{NO}}$ (cm <sup>-1</sup> ) <sup>c</sup>	I/O vs NHE (V, E <sub>p,a</sub> ) <sup>d</sup>
1	W		1546	0.50
2	W		1546	0.44 (2A) 0.46 (2B)
3	W		1554	--
5	W		1552	--
6	W		1546	-0.20 <sup>a</sup>
7	Mo		1574	0.18
9	Mo		1571	0.27
10	Mo		1558	-0.64 <sup>a</sup>
4	W	CO	1580	0.32 <sup>b</sup>
8	Mo	CO	1583	0.22

<sup>a</sup>  $\eta^1$  complex in solution shifts E<sub>p,a</sub> negative. <sup>b</sup> E<sub>1/2</sub>. <sup>c</sup> HATR (glaze). <sup>d</sup> 100 mV/s; DMA/TBAH.

Owing to the chiral nature of the metal fragment and the high metal–carbonyl rotational barrier, the tungsten acetaldehyde complex TpW(NO)(PMe<sub>3</sub>)( $\eta^2$ -acetaldehyde) (**1**) was isolated as a mixture of three isomers. <sup>1</sup>H NMR spectra of the crude mixture showed a ratio of 2:5:1 (A:B:C). Over the course of 4 days at 70 °C, the latter isomer (C) diminished, and isomers A and B reached a 1:2 equilibrium.<sup>20</sup>

To facilitate the identification of coordination diastereoisomers, a quadrant designation was used.<sup>21–23</sup> In all cases, the C=O bond is parallel to the M–L bond (L = PMe<sub>3</sub> or MeIm).<sup>24</sup> Looking from carbonyl to tungsten such that the NO is on the right, the PMe<sub>3</sub> is up, and the Tp extends to the lower left, four quadrants are designated according to Scheme 1.

Using preparatory TLC, small quantities of the primary (**1B**) and secondary (**1A**) isomer were isolated and assigned with the aid of NOE data. The primary isomer (**1B**) has the carbonyl oxygen pointing away from the PMe<sub>3</sub> with the methyl group extended into quadrant d, while the secondary isomer has the oxygen toward the PMe<sub>3</sub> with the methyl in quadrant a (**1A**) (Table 2). The minor isomer C is assigned to be a thermodynamically

**Scheme 1****Table 2. Observed  $\eta^2$  Diastereoisomers of {TpW(NO)(PMe<sub>3</sub>)(L)}<sup>a</sup>**

Complex	A	B	C
1			
		20 : 40	<1 <sup>a</sup>
2			
		>10 : 1 <sup>a</sup>	
3			
		1 : 2	1 <sup>a</sup>
5			
		1 : 1 <sup>a</sup>	
6			
		1 : 2 <sup>b</sup>	

<sup>a</sup> Thermodynamic ratio: (a) @ 22 °C; (b) @ -60 °C.

ally unstable rotamer of B. The aldehyde signal for all three diastereoisomers is found significantly upfield from that of a free aldehyde (e.g., from 9.72 to 4.30 ppm for **1B**, and 2.84 for **1A**). <sup>13</sup>C NMR data also showed the expected upfield shift of the bound carbons (e.g., from

(20) This ratio did not change after another 7 days of heating at 70 °C.

(21) Meiere, S. H.; Harman, W. D. *Organometallics* **2001**, *20*, 3876–3883.

(22) Crocco, G. L.; Lee, K. E.; Gladysz, J. A. *Organometallics* **1990**, *9*, 2819–2831.

(23) Tam, W.; Wong, W. K.; Gladysz, J. A. *J. Am. Chem. Soc.* **1979**, *101*, 1, 1589–1591.

(24) Gunnoe, T. B.; Sabat, M.; Harman, W. D. *Organometallics* **2000**, *19*, 728–740.

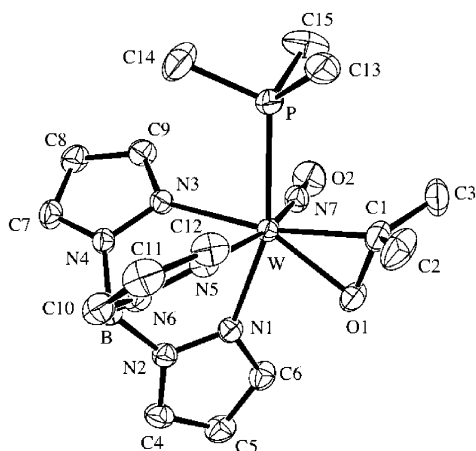


**Figure 1.** ORTEP diagram of the acetone complex **2B** (30% ellipsoids). Selected bond lengths (Å): W–O(1), 2.040(2); W–C(1), 2.213(3); W–N(7), 1.766(2); W–P, 2.5122(8); O(1)–C(1), 1.354(4). Bond angles (deg): O(1)–W–C(1), 36.86(10); O(1)–C(1)–C(3), 115.1(3); O(1)–C(1)–C(2), 112.2(4); C(3)–C(1)–C(2), 112.7(4).

199 to 85.2 ppm for **1B**), and for the bound carbon that eclipses the phosphorus (**1B**), a doublet ( $J_{PC} = 17$  Hz) was observed.

In a similar manner, other tungsten carbonyl complexes **2–6** were prepared, isolated, and stereochemically assigned, and these results are summarized in Table 2.

The tungsten-acetone complex,  $\text{TpW}(\text{NO})(\text{PMe}_3)(\eta^2\text{-acetone})$  (**2**), upon its formation, crystallizes out of acetone solution, and a single crystal of this material was characterized by X-ray diffraction. The molecular diagram of **2** shows the bound acetone in an unexpected geometry, with its methyls oriented toward the  $\text{PMe}_3$  (Figure 1). This places a methyl group into the sterically encumbered quadrant c.<sup>21</sup> However, when this isomer (**2B**) is heated in THF in a sealed tube (90 °C) overnight,  $^1\text{H}$  NMR data indicate the conversion of **2B** to its diastereomer **2A**, with the acetone methyl groups now away from the  $\text{PMe}_3$  (Table 2).

The reaction of  $\text{TpW}(\text{NO})(\text{PMe}_3)(\eta^2\text{-benzene})$  with methyl formate yielded three diastereomers of  $\text{TpW}(\text{NO})(\text{PMe}_3)(\eta^2\text{-methyl formate})$ , **3A–3C**, along with two other products (**4** and **3H**). One of these side products (**4**) featured a M–CO stretching frequency at  $1864\text{ cm}^{-1}$  (cf.  $\text{TpMo}(\text{NO})(\text{MeIm})(\text{CO})$ :  $\nu(\text{CO}) = 1865\text{ cm}^{-1}$ ) and a relatively high-energy nitrosyl stretching frequency at  $1580\text{ cm}^{-1}$ . On this basis we assign **4** to be  $\text{TpW}(\text{NO})(\text{PMe}_3)(\text{CO})$ . A  $^{13}\text{C}$  resonance at 251.1 ppm and a reversible couple for the complex at +0.32 V (cf.  $\text{TpMo}(\text{NO})(\text{MeIm})(\text{CO})$ : 0.08 V) further support this assignment. Interestingly, attempts to synthesize this CO complex directly from  $\text{TpW}(\text{NO})(\text{PMe}_3)(\eta^2\text{-benzene})$  and CO (40 psi) failed. The other byproduct, **3H**, shows a hydride doublet at 12.6 ppm ( $J_{\text{PH}} = 129$  Hz), a formate proton at 8.60 ppm, and a  $m/z = 548$  (FAB) consistent with the formulation  $\text{TpW}(\text{NO})(\text{PMe}_3)\cdot\text{HCOOH}$ . Infrared data include a nitrosyl stretch at  $1592\text{ cm}^{-1}$ , a carbonyl stretch at  $1627\text{ cm}^{-1}$ , and a weak  $\nu(\text{WH}) = 1867\text{ cm}^{-1}$ . Taken together, these data confirm the formation of  $\text{TpW}(\text{NO})(\text{PMe}_3)(\text{H})(\text{O}_2\text{CH})$ , the oxidative addition product of  $\text{TpW}(\text{NO})(\text{PMe}_3)$ , and adventitious formic acid (vide infra).

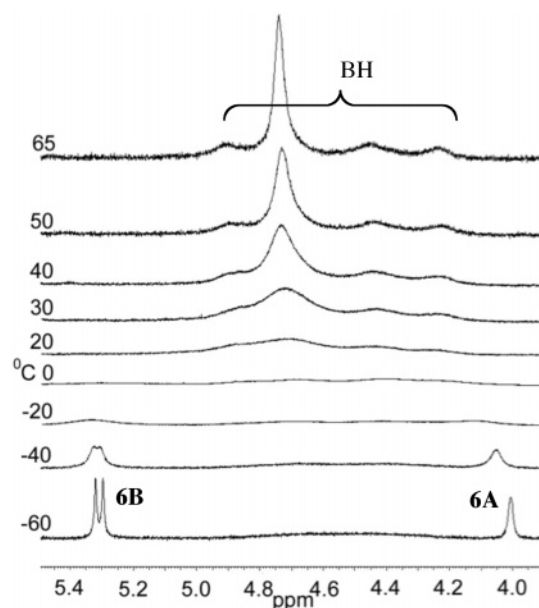


**Figure 2.**  $^1\text{H}$  NMR spectra of  $\text{TpW}(\text{NO})(\text{PMe}_3)(\eta^2\text{-DMF})$  **6** at various temperatures.

The ethyl acetate complex  $\text{TpW}(\text{NO})(\text{PMe}_3)(\eta^2\text{-ethyl acetate})$  (**5**) could not be prepared by the usual method (neat ethyl acetate), but was ultimately isolated as a 1:1 mixture of isomers (**5A** and **5B**) from a pentane suspension of  $\text{TpW}(\text{NO})(\text{PMe}_3)(\eta^2\text{-benzene})$  containing a small amount of the ester. A crude sample of **5** was characterized by  $^1\text{H}$  and  $^{13}\text{C}$  NMR,  $^{31}\text{P}$  NMR, and IR data. The carbonyl  $^{13}\text{C}$  signal for one of the two isomers (**B**) shows significant coupling (22 Hz) with phosphorus, suggesting that for this isomer the oxygen points away from the phosphorus. Isomer **5A** can be differentiated from **5B** by the highly shielded methyl group for the former (1.01 ppm), a phenomenon that is associated with the methyl projecting into quadrant b.<sup>21</sup> As with the formate analogue, a byproduct of this reaction was the oxidative addition complex  $\text{TpW}(\text{NO})(\text{PMe}_3)(\text{H})(\text{OAc})$ , **5H** (vide infra). Attempts to purify the ester complexes by chromatography on  $\text{SiO}_2$  gave only **5H**.

The tungsten DMF complex  $\text{TpW}(\text{NO})(\text{PMe}_3)(\eta^2\text{-DMF})$ , **6**,<sup>14</sup> undergoes rapid coordination isomerization at ambient temperatures. Proton data show a single resonance corresponding to the amide methyl groups and a broad resonance assigned to the formyl proton. Upon cooling (Figure 2), the formyl peak broadens, eventually yielding two signals, a doublet and a singlet half its size. The doublet, corresponding to the formyl proton of complex **6B** (Table 2), features a large phosphorus coupling ( $J_{\text{PH}} = 12$  Hz), which has been routinely observed in related complexes for the proton of the bound carbon that eclipses the  $\text{PMe}_3$ .<sup>24</sup> The amide methyl resonance also resolves into two separate peaks upon cooling.  $^{13}\text{C}$  NMR data for the major isomer **6B** includes a doublet ( $J_{\text{PC}} = 19$  Hz) at 110.0 ppm corresponding to the bound carbonyl.

Cyclic voltammetric data for **6** were unusually sensitive to scan rate. The anodic peak near  $-300$  mV (NHE) was severely broadened at 100 mV/s, and at 20 mV/s this feature was completely absent (Figure 3). When the scan rate was increased to 2000 mV/s, the anodic peak shifted positive, approaching values seen for other  $\eta^2$  carbonyl complexes (Table 1). A return sweep revealed



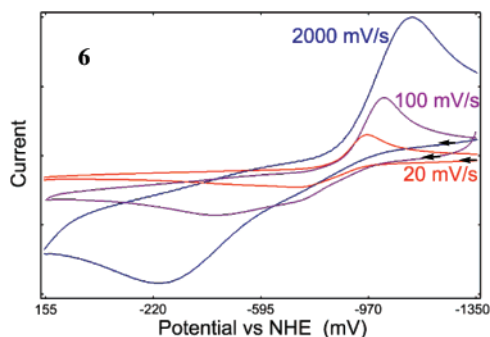
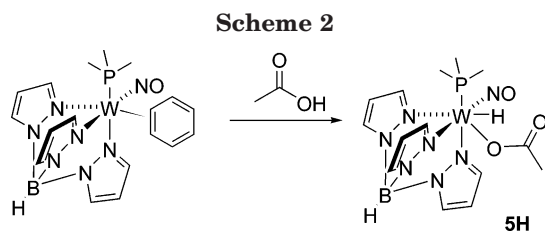


**Figure 3.** Cyclic voltammogram of  $\text{TpW}(\text{NO})(\text{PMe}_3)(\eta^2\text{-DMF})$  **6** at various scan rates.

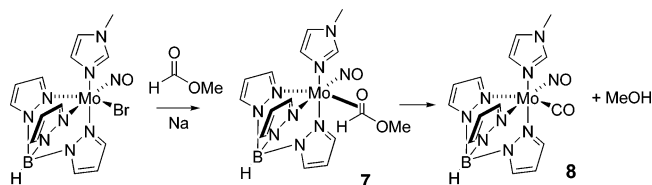


a cathodic wave near  $-1$  V for the full range of scan rates (20–2000 mV/s; see discussion). IR did not indicate the presence of any tungsten(I) complexes; the only visible nitrosyl stretch occurred at  $1546\text{ cm}^{-1}$ . Heating a DMF solution of **6** at  $90^\circ\text{C}$  for 4 h effected its conversion to **4**, the same decarbonylation product derived from methyl formate. Attempts to identify either an  $\eta^2$ -amide or CO complex from acetamide were unsuccessful.

In an attempt to observe an  $\eta^2$ -coordinated carboxylic acid, the tungsten benzene complex was dissolved in acetic acid and allowed to stand for 3 h. After isolation, proton data revealed the formation of the hydride  $\text{TpW}(\text{NO})(\text{PMe}_3)(\text{H})(\text{OAc})$ , **5H**, the oxidative addition product first observed as a byproduct from ethyl acetate (vide supra; Scheme 2). The  $^1\text{H}$  NMR spectrum of **5H** showed the metal hydride resonance as a doublet at 13.22 ppm with a P–H coupling constant of 130 Hz, consistent with other seven-coordinate tungsten hydrides.<sup>25,26</sup> In addition to the doublet,  $^{183}\text{W}$  satellites (14%) about the doublet were present in the spectrum, appearing as a doublet of doublets ( $J_{\text{WH}} = 13$  Hz). Infrared data showed a W–H band for **5H** at  $1891\text{ cm}^{-1}(\text{w})$ . Upon exposure of the complex to  $\text{D}_2\text{O}$  for 30 min, this feature, as well as the proton resonance disappeared.

The  $\{\text{TpMo}(\text{NO})(\text{MeIm})\}$  fragment has proven to be a powerful  $\pi$  base,<sup>18,19</sup> similar to its heavy metal congener. Thus, we endeavored to prepare representative carbonyl complexes for this system for the purpose of comparison. The best synthetic route to  $\text{TpMo}(\text{NO})(\text{MeIm})(\text{L})$  complexes involves the reduction of a  $\text{Mo}(\text{I})$  precursor in the presence of an excess of L.<sup>18,19</sup> The preparation of a molybdenum acetaldehyde complex was attempted by reducing  $\text{TpMo}(\text{NO})(\text{MeIm})\text{Br}$  with sodium in the presence of an excess of the aldehyde, but this reaction was unsuccessful. The molybdenum acetone complex  $\text{TpMo}(\text{NO})(\text{MeIm})(\eta^2\text{-acetone})$ , **9**, was

**Scheme 3**



first successfully prepared via a substitution procedure and isolated as a single isomer analogous to **2A**.<sup>18</sup> An alternate synthesis incorporating the sodium reduction of  $\text{TpMo}(\text{NO})(\text{MeIm})\text{Br}$  in the presence of acetone is reported in the Experimental Section (67%).

When a THF solution of  $\text{TpMo}(\text{NO})(\text{MeIm})\text{Br}$  and methyl formate was reduced with sodium dispersion, a mixture of the anticipated dihapto-bound formate (**7**) and its decarbonylated product  $\text{TpMo}(\text{NO})(\text{MeIm})(\text{CO})$  (**8**) was obtained. The formate complex has an IR nitrosyl stretching frequency of  $1574\text{ cm}^{-1}$ , similar to the ketone analogue **9**. The (I/O) oxidation wave for the complex appears to be at  $E_{\text{p,a}} = +180$  mV and is partially obscured by the (I/O) oxidation wave for  $\text{TpMo}(\text{NO})(\text{MeIm})(\text{CO})$ . Proton and carbon NMR data for **7** are consistent with a dihapto-bound ester, including a carbon resonance for the bound CO at 161.7 ppm. Attempts to isolate this complex in pure form failed as a result of its tendency to undergo decarbonylation (Scheme 3).<sup>19</sup> However, the molybdenum DMF complex  $\text{TpMo}(\text{NO})(\text{MeIm})(\eta^2\text{-DMF})$ , **10**, was successfully obtained (35%) by reduction of  $\text{TpMo}(\text{NO})(\text{MeIm})\text{Br}$  in an excess of DMF. This amide complex has similar properties to its tungsten congener, featuring a nitrosyl stretching frequency at  $1558\text{ cm}^{-1}$ , a broadened formyl proton resonance at 4.97 ppm, and a methyl signal at 2.63 ppm. When an acetone- $d_6$  solution of **10** is cooled to  $-90^\circ\text{C}$ , the signals at 4.97 and 2.63 ppm sharpen, but do not split. These data indicate that while this complex is most likely fluxional at ambient temperatures, in this case, one stereoisomer dominates. Without the aid of definitive NOE or phosphorus coupling data, an accurate assignment of stereochemistry for **10** is difficult. However, in consideration of the stereochemical preferences observed for the analogous rhenium compounds  $\text{TpRe}(\text{CO})(\text{MeIm})(\eta^2\text{-L})$  (L = a ketone, aldehyde, or ester), which uniformly favor the oxygen up toward the imidazole, we can tentatively assign the stereochemistry for **10** as being analogous to **6A**. Cyclic voltammetric data for **10** were virtually identical to those collected for the tungsten analogue (Figure 3), where the anodic wave varied widely with changes in scan rate. Surprisingly, the known compound  $\text{TpMo}(\text{NO})(\text{MeIm})(\text{CO})$  was not observed as a decomposition product of **10**. Heating **10** in an acetone- $d_6$  solution yields the acetone complex (**9-d<sub>6</sub>**), free DMF, and several unidentified products.

## Discussion

The  $\{\text{TpW}(\text{NO})(\text{PMe}_3)\}$  and  $\{\text{TpMo}(\text{NO})(\text{MeIm})\}$  fragments have an exceptional ability to disrupt delocalized  $\pi$  systems through dihapto coordination.<sup>14,19</sup> In this regard, they are similar to the  $\{\text{TpRe}(\text{CO})(\text{MeIm})\}$  and  $\{\text{Os}(\text{NH}_3)_5\}^{2+}$  fragments. For example, each of the three heavy metal systems form unusually stable  $\eta^2$ -benzene

(25) Chisholm, M. H.; Eichhorn, B. W.; Huffman, J. C. *J. Chem. Soc., Chem. Commun.* **1985**, 861–863.

(26) Caffyn, A. J. M.; Feng, S. G.; Dierdorf, A.; Gamble, A. S.; Eldredge, P. A.; Vossen, M. R.; White, P. S.; Templeton, J. L. *Organometallics* **1991**, *10*, 2842–2848.

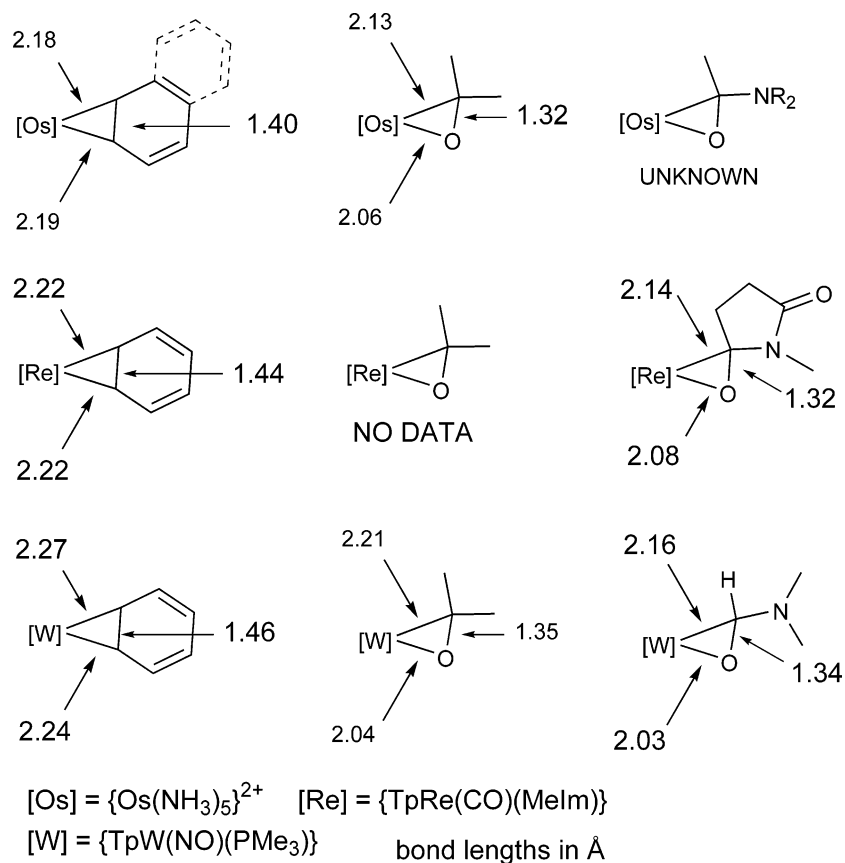


**Figure 4.** Bond distances for various  $\eta^2$  complexes.

complexes with similar half-lives of arene displacement ( $\sim 4$  h at 20 °C).<sup>14,27,28</sup> This similarity is reiterated by the near match in electrochemical potentials ( $\sim 200$  mV, NHE) and inner sphere coordination geometries for these d<sup>6</sup> systems. In Figure 4, structural information is presented for  $\eta^2$ -arene,  $\eta^2$ -acetone, and  $\eta^2$ -amide complexes. A comparison of bond lengths for W, Re, and Os arenes shows a significant lengthening in the bound C–C bond going from Os to Re to W. This trend is consistent with increased back-bonding into an arene  $\pi^*$  orbital and is exemplified by the data available for  $\eta^2$ -carbonyl complexes as well, the C–O bond length reaching its maximum for tungsten. Dihapto-coordinated ester and amide complexes are observed for both rhenium and tungsten, whereas osmium forms only  $\eta^2$ -aldehyde and ketone complexes. While the rhenium fragment also forms complexes with the pseudo amides succinimide and *N*-acetylpyrrole,<sup>13</sup> the purported adducts of DMF<sup>29</sup> and *N*-methylacetamide<sup>13</sup> rapidly decarbonylate to give the CO complex TpRe(CO)<sub>2</sub>(MeIm). Similarly rapid decarbonylation is seen with pentaammineosmium(II).<sup>16</sup> The tungsten fragment's ability to successfully back-bond into the high-energy  $\pi^*$  orbital of an amide highlights its superior  $\pi$  basicity compared to the rhenium and osmium fragments.

Prevailing wisdom might argue that decarbonylation of aldehydes, formates, and formamides requires an

electron-rich transition metal in order to competently carry out the oxidative addition of the OC–H bond.<sup>30–32</sup> It is at first curious, then, that the rate of decarbonylation of an  $\eta^2$ -amide complex across the Os–Re–W series is *inversely dependent* on the back-bonding ability of the metal. Whereas the tungsten complex **6** is easily isolated, the purported DMF complexes for Re and Os immediately give way to the corresponding CO complex.<sup>16</sup> The molybdenum analogue **10**, similar to **6**, is kinetically stable to decarbonylation. However, these observations are consistent with the notion that the  $\eta^2$ -amide complex is not on the reaction path for decarbonylation. Rather,  $\eta^2$ -coordination is a kinetic “dead end” that must be reversed in order to achieve oxidative addition of the C–H bond. The analogous situation is often the case for C–H activation of alkenes.<sup>33</sup>

Decarbonylation of aldehydes,<sup>31,34–37</sup> formates,<sup>38,39</sup> and formamides<sup>39,40</sup> has been extensively studied. Typically, proposed mechanisms involve an oxidative addi-

(30) Crabtree, R. H. *The Organometallic Chemistry of the Transition Metals*; Wiley: New York, 2001.

(31) Beck, C. M.; Rathmill, S. E.; Park, Y. J.; Chen, J.; Crabtree, R. H.; Liable-Sands, L. M.; Rheingold, A. L. *Organometallics* **1999**, *18*, 5311–5317.

(32) Collman, J. P.; Hegedus, L. S.; Norton, J. R.; Finke, R. G. XXXXX; University Science Books: Mill Valley, CA, 1987.

(33) Stoutland, P. O.; Bergman, R. G. *J. Am. Chem. Soc.* **1985**, *107*, 4581–4582.

(34) Barrio, P.; Esteruelas, M. A.; Onate, E. *Organometallics* **2004**, *23*, 1340–1348.

(35) Abu-Hasanayn, F.; Goldman, M. E.; Goldman, A. S. *J. Am. Chem. Soc.* **1992**, *114*, 2520–2524.

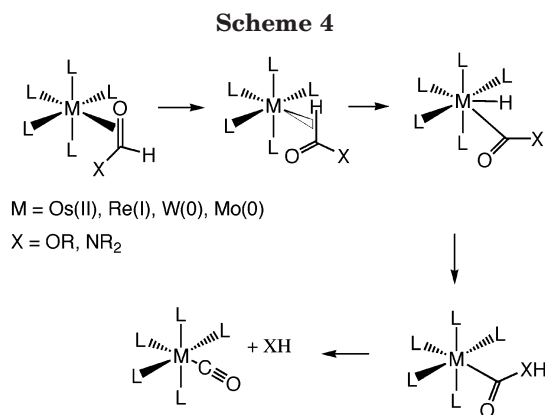
(36) Alaimo, P. J.; Arndtsen, B. A.; Bergman, R. G. *Organometallics* **2000**, *19*, 2130–2143.

(37) Gupta, P.; Basuli, F.; Peng, S.-M.; Lee, G.-H.; Bhattacharya, S. *Indian J. Chem., Sect. A: Inorg., Bio-inorg., Phys., Theor. Anal. Chem.* **2003**, *42*, 2406–2415.

(27) Harman, W. D. *Chem. Rev.* **1997**, *97*, 1953–1978.

(28) Meiere, S. H.; Brooks, B. C.; Gunnoe, T. B.; Sabat, M.; Harman, W. D. *Organometallics* **2001**, *20*, 1038–1040.

(29) Attempts to prepare the Re DMF complex (this work) by established methods resulted in quantitative formation of the CO complex, similar to that reported for *N*-methylformamide in ref 13.



tion of either the C–H or C–X bond ( $X = \text{OR}$  or  $\text{NR}_2$ ) and a deinsertion step to form the M–CO. Usually, transition metal complexes that are competent decarbonylation agents are coordinatively unsaturated or have alkyl or hydride ligands that can reductively eliminate with either X or H. Given the high coordination number of the  $\text{ML}_5$  systems discussed in this study, we speculate that the mechanism for decarbonylation of formamides and formates involves a direct elimination of XH from the carbonyl, thereby avoiding an unreasonable coordination number. In Scheme 4, the  $\eta^2$ -ester or amide must first form a sigma complex (shown) or other form (e.g., O-bound) that leads to oxidative addition (vide infra). A proton is then transferred from the metal to the X group. Finally the XH group is eliminated (the reverse of nucleophilic addition to MCO) to form the decarbonylation product.

That the tungsten-promoted decarbonylation is a more facile process for amides and esters (20 °C) than it is for aldehydes (>70 °C) runs counter to what was reported by Caulton et al. for a coordinatively unsaturated ruthenium system,<sup>39</sup> but is consistent with a change in mechanism. Our observations with  $\{\text{TpRe}(\text{CO})(\text{MeIm})\}$  and  $\{\text{Os}(\text{NH}_3)_5\}^{2+}$  mirror the observations for tungsten: For osmium, decarbonylation of DMF is complete in a matter of seconds, while the  $\eta^2$ -aldehyde complex has a half-life of 16 h in acetonitrile at 20 °C.<sup>16</sup> The complex  $\text{TpRe}(\text{CO})(\text{MeIm})(\eta^2\text{-acetaldehyde})$  is stable at this temperature, while the putative DMF complex, prepared from the benzene analogue<sup>28</sup> and DMF, over the course of 24 h at 20 °C yields only  $\text{TpRe}(\text{CO})_2(\text{MeIm})$ .<sup>13,41</sup>

**Stereochemistry.** In general, the  $\text{TpW}(\text{NO})(\text{PMe}_3)$  carbonyl complexes reported herein are formed as mixtures of two or more stereoisomers (see Table 2). Only in the case of  $L = \text{acetone}$  is one isomer (**A**) overwhelmingly favored at equilibrium, and in this case, it is the *other* possible isomer (**B**) that precipitates from acetone solution. For the rhenium and molybdenum imidazole complexes  $\{\text{TpRe}(\text{CO})(\text{MeIm})(\text{carbonyl})\}$  and  $\{\text{TpMo}(\text{NO})(\text{MeIm})(\text{carbonyl})\}$ , coordination stereochemistry is typically selective, the dominant isomer(s) being that which does not place a substituent in quadrant

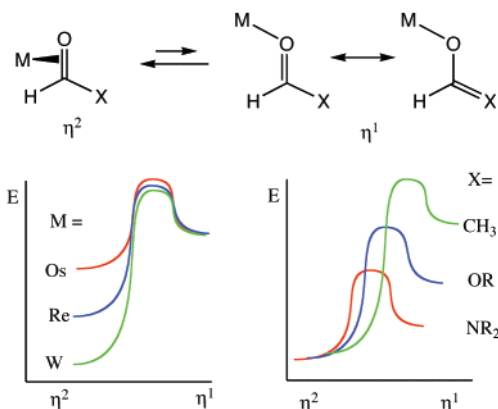


**Figure 5.** Relative activation barriers for the  $\eta^2$  to  $\eta^1$  isomerization of carbonyl ligands.

c.<sup>13,21</sup> This observation was rationalized by invoking a steric interaction ( $\sim 10$  kcal) between that substituent (or even hydrogen)<sup>21</sup> and the pyrazole ring trans to the CO.<sup>21</sup> While this feature is still present in the tungsten systems, it is clearly less pronounced (see Table 2). One important difference is the phosphine ligand, which consistently forces a lengthening in the W–C or W–O bond that eclipses it (see Figure 4). A similar distortion was observed for the complexes of the type  $\text{TpRe}(\text{CO})(\text{PMe}_3)(\text{alkene})$ .<sup>24,42</sup> While this distortion is surely due to a steric interaction between the phosphine ligand and the  $\pi$ -bound ligand, this geometric distortion apparently relieves much of the steric interaction between a substituent of the  $\pi$ -bound ligand and the pyrazole ring extending into quadrant c. Consider the ethyl acetate complex **5**, which shows a 1:1 equilibrium ratio of **A** and **B**.

**$\eta^2$  to  $\eta^1$  Isomerization.** The complex  $[\text{Os}(\text{NH}_3)_5(\eta^2\text{-acetone})]^{2+}$  undergoes an  $\eta^2$  to  $\eta^1$  isomerization at ambient temperature with a specific rate of about  $1 \text{ s}^{-1}$ .<sup>43</sup> The corresponding rhenium and tungsten complexes also undergo this process, but at a much slower rate.<sup>21</sup> However, for esters, amides, and pseudo-amides, the  $\eta^2$  to  $\eta^1$  isomerization becomes much faster, giving rise to  $^1\text{H}$  NMR spectra with severe broadening at room temperature.<sup>13</sup> In contrast, the tungsten ester complexes **3** and **5** appear static on the NMR time scale. However, the amide complex **6** is fluxional, with a rate to isomerization measured as  $1.5 \times 10^3 \text{ s}^{-1}$  at 0 °C.<sup>14</sup> For the molybdenum analogue **10**, the rate of isomerization is even faster. Broadening is observable in the  $^1\text{H}$  NMR spectrum for **10** even at  $-50$  °C, but an  $\eta^2$  to  $\eta^1$  isomerization rate could not easily be measured given that only one stereoisomer is present at  $-90$  °C. Similar dynamics were observed for the complex  $\text{TpRe}(\text{CO})(\text{MeIm})(\text{EtOAc})$ .<sup>13</sup> In summary, as the  $\pi$  interaction in the  $\eta^1$ -bound isomer between the carbonyl and substituent increases ( $\text{CH}_3 \ll \text{OR} < \text{NMe}_2$ ), this isomer becomes more energetically competitive with the  $\eta^2$  form (Figure 5) and is more easily accessed (i.e., there is a lower activation barrier for  $\eta^2$  to  $\eta^1$  isomerization). The greater back-bonding present as one moves from osmium to rhenium to tungsten raises this barrier by further stabilizing the  $\eta^2$ -bound isomer.

(38) Zahalka, H. A.; Alper, H.; Sasson, Y. *Organometallics* **1986**, *5*, 2497–2499.

(39) Coalter, J. N. I.; H., J. C.; Caulton, K. G. *Organometallics* **2000**, *19*, 3569–3578.

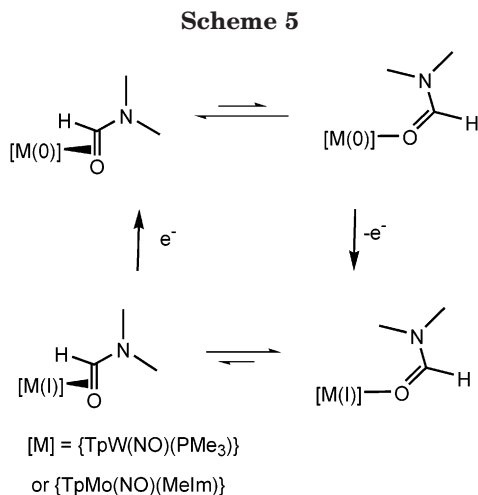
(40) van der Rest, G.; Mourgues, P.; Nedev, H.; Audier, H. E. *J. Am. Chem. Soc.* **2002**, *124*, 5561–5569.

(41) This work. For characterization of the CO complex, see the following reference.

(42) Gunnoe, T. B.; Sabat, M.; Harman, W. D. *J. Am. Chem. Soc.* **1999**, *121*, 6499–6500.

(43) Harman, W. D.; Sekine, M.; Taube, H. *J. Am. Chem. Soc.* **1988**, *110*, 2439–2445.





The  $d^5/d^6$  reduction potentials observed by cyclic voltammetry for tungsten are, in general, more positive (i.e., more difficult to oxidize) than those for their rhenium and molybdenum analogues. This highlights a paradoxical property of the {TpW(NO)(PMe<sub>3</sub>)} fragment. While, this metal fragment is more  $\pi$ -basic than its rhenium or molybdenum counterpart, {TpRe(CO)(MeIm)}, it is marginally less reducing as judged by electrochemical data. The  $\eta^2$  to  $\eta^1$  isomerization and its reverse play a prominent role in the cyclic voltammetry of the DMF complexes of tungsten (**6**) and molybdenum (**10**) (see Figure 3). Whereas the tungsten and molybdenum aldehyde, ketone, and ester complexes show oxidation waves from 0.27 to 0.44 V at 100 mV/s, slightly positive compared to those observed for arenes, the oxidation waves of the amide complexes are practically indiscernible. Only at high scan rates can a severely broadened wave be readily observed (see Figure 3). This is consistent with a  $C_rE_r$  mechanism<sup>44</sup> (Scheme 5), in which an  $\eta^2$  to  $\eta^1$  isomerization occurs at low scan rates, followed by oxidation of the more reducing  $\eta^1$  isomer (presumably, *O*-bound). The reduction of the latter species is in turn signaled by a reduction wave near -1.0 V, rendered irreversible by a proceeding  $\eta^1$  to  $\eta^2$  isomerization. A similar cycle was observed for  $\eta^2$  ketone complexes of osmium(II).<sup>43</sup>

**Tungsten Hydride.** The oxidative addition of tungsten across formic and acetic acids produces thermally stable, seven-coordinate tungsten(II) hydride complexes. Although hydride signals appearing far downfield (ca. 13 ppm) are uncommon, they have been observed as high as 20.4 ppm for tungsten hydrides.<sup>25</sup> For example, the complex Tp\*W(CO)(PhCCMe)H shows a hydride signal at 10.8 ppm.<sup>26</sup> The <sup>183</sup>W-H coupling ( $J^{183}_{WH} = 13$  Hz) observed for **5H** is also unusually low, indicating a long W-H bond,<sup>45</sup> similar to that observed for the seven-coordinate complex Tp\*W(CO)<sub>3</sub>H ( $J^{183}_{WH} = 9$  Hz).<sup>26</sup> The hydride also shows a large phosphorus coupling ( $J_{PH} = 130$  Hz), similar to the complex Cp\*W(NO)(H)(PMe<sub>3</sub>)(C<sub>6</sub>H<sub>4</sub>PPh<sub>2</sub>), which has a  $J_{PH}$  coupling constant of 94 Hz.<sup>12</sup> Such large coupling constants generally indicate the hydride is *cis* to the phosphine (the unusual complex Cp\*W(NO)(H)( $\eta^2$ -PPh<sub>2</sub>C<sub>6</sub>H<sub>4</sub>) ori-

ents the hydride *trans* to the phosphorus and consequently has a  $J_{PH}$  of only 10 Hz).<sup>46</sup> MS data and the acetate chemical shift in the <sup>1</sup>H NMR spectrum indicate that this anion is bound to the metal, and not a counterion. The NO stretch at 1580 cm<sup>-1</sup> is significantly higher than expected for an  $\eta^2$  carboxylic acid complex (Table 2), and the acetate CO stretch is consistent with the acetate coordinated in the conventional  $\eta^1$  (oxygen bound) mode. Significantly, the B-H stretch (2490 cm<sup>-1</sup>) of **5H** is nearly identical to that of TpW(NO)(PMe<sub>3</sub>)( $\eta^2$ -benzene) (2484 cm<sup>-1</sup>), which supports the hypothesis that the Tp ligand in **5H** is fully chelated ( $\kappa^3$ ). The B-H stretch is very sensitive to changes in hapticity of the Tp ligand and would shift to higher frequency upon dechelation of a Tp arm<sup>47</sup> (cf. TpRu(H)(CS)(PPh<sub>3</sub>), 2480 cm<sup>-1</sup> vs ( $\kappa^2$ -HB(pz)<sub>3</sub>)Ru(H)(CS)(PPh<sub>3</sub>)<sub>2</sub>, 2435 cm<sup>-1</sup>).<sup>48</sup> Attempts to synthesize other hydride complexes from simple Brønsted acids (water, alcohols, amines, HX) failed to produce other isolable hydride complexes.<sup>49</sup>

## Experimental Section

**General Methods.** NMR spectra were obtained on a 300 or 500 MHz Varian INOVA spectrometer. All chemical shifts are reported in ppm and are referenced to tetramethylsilane (TMS) utilizing residual <sup>1</sup>H or <sup>13</sup>C signals of the deuterated solvents as an internal standard. Phosphorus resonances are referenced to phosphoric acid. Coupling constants ( $J$ ) are reported in hertz (Hz). Resonances in the <sup>1</sup>H NMR due to pyrazole ligands (Tp) are listed by chemical shift and multiplicity only (all coupling constants are 2 Hz). Infrared spectra (IR) were recorded on a MIDAC Prospect Series (Model PRS) spectrometer as a glaze on a horizontal attenuated total reflectance (HATR) accessory (Pike Industries). Electrochemical experiments were performed under a dinitrogen atmosphere using a BAS Epsilon EC-2000 potentiostat. Cyclic voltammetry data were taken at ambient temperature at 100 mV/s (25 °C) (unless otherwise specified) in a standard three-electrode cell from +1.7 to -1.7 V with a glassy carbon working electrode, *N,N*-dimethylacetamide (DMA) solvent, and tetrabutylammoniumhexafluorophosphate (TBAH) electrolyte (~0.5 M). All potentials are reported versus NHE (normal hydrogen electrode) using cobaltocenium hexafluorophosphate ( $E_{1/2} = -0.78$  V) or ferrocene ( $E_{1/2} = 0.55$  V) as an internal standard. The peak-to-peak separation was less than 100 mV for all reversible couples. Mass spectra were obtained on either a JEOL JMS600 using FAB<sup>+</sup> or a Finnigan MAT TSQ7000 using ESI<sup>+</sup>; no counterions were observed. Elemental analyses were performed with a Perkin-Elmer 2400 Series II CHNS/O analyzer or obtained from Atlantic Microlabs, Inc. Unless otherwise noted, all synthetic reactions and electrochemical experiments were performed under a dry nitrogen atmosphere. CH<sub>2</sub>Cl<sub>2</sub>, benzene, THF (tetrahydrofuran), and hexanes were purged with nitrogen and purified by passage through a column packed with activated alumina. Other solvents and liquid reagents were thoroughly purged with nitrogen prior to use. Deuterated solvents were used as received from Cambridge Isotopes. Sodium amalgam (1.0 wt %), a viscous liquid, was prepared by slowly adding small pieces of sodium to mercury under an inert atmosphere. Compounds **6**,<sup>14</sup> **8**,<sup>19</sup> and **9**<sup>18</sup> have been reported previously.

(46) Debad, J. D.; Legzdins, P.; Lumb, S. A. *Organometallics* **1995**, *14*, 2543-2555.

(47) Akita, M.; Ohta, K.; Takahashi, Y.; Hikichi, S.; Moro-oka, Y. *Organometallics* **1997**, *16*, 4121-4128.

(48) Burns, I. D.; Hill, A. F.; White, J. P. A.; Williams, D. J.; Wilton-Ely, J. D. E. *Organometallics* **1998**, *17*, 1552-1557.

(49) NMR evidence for hydride formation has been obtained in the reaction of the tungsten benzene complex with some anilines.

(44) Bard, A. J.; Faulkner, L. R. *Electrochemical Methods Fundamentals and Applications*; John Wiley & Sons: New York, 1980.

(45) Legzdins, P.; Martin, J. T.; Einstein, F., W. B.; Willis, A. C. *J. Am. Chem. Soc.* **1986**, *108*, 7971-7981.

**TpW(NO)(PMe<sub>3</sub>)( $\eta^2$ -acetaldehyde) (1).** TpW(NO)(PMe<sub>3</sub>)-( $\eta^2$ -benzene) (222 mg, 0.383 mmol) was dissolved in 2 mL of DME. Into this solution 1.5 mL of acetaldehyde was added and the reaction mixture sat for 3 h (20 °C). The reaction mixture was added to pentane and collected on a medium-porosity frit, washed with pentane, and dried in vacuo to give **1** (134.8 mg, 0.2464 mmol, 64% yield) (all three diastereomers) as a brown powder. IR (HATR glaze):  $\nu_{\text{NO}} = 1546 \text{ cm}^{-1}$ . CV (DMA, TBAH, 100 mV/s, vs NHE):  $E_{\text{p,a}} = +0.50 \text{ V}$ . FAB-MS:  $m/z = 547 [\text{M}]^+$ . <sup>31</sup>P NMR (acetone-*d*<sub>6</sub>,  $\delta$ ): -8.10 (satellite d ( $J = 300.3$ ) PMe<sub>3</sub>). Anal. Calcd for C<sub>14</sub>H<sub>23</sub>WPO<sub>2</sub>N<sub>7</sub>B: C, 30.74; H, 4.24; N, 17.94. Found: C, 30.26; H, 4.35; N, 17.99. Small yields of the primary (2.1 mg) and secondary diastereomers (5.7 mg) were isolated after prep TLC on a 1000  $\mu\text{m}$  alumina plate (eluted with 1:1 THF/Et<sub>2</sub>O) and used for the following characterization. Primary diastereomer (**1B**): <sup>1</sup>H NMR (acetone-*d*<sub>6</sub>,  $\delta$ ): 8.17 (1H, d, Tp), 8.09 (1H, d, Tp), 8.03 (1H, d, Tp), 7.84 (1H, d, Tp), 7.78 (1H, d, Tp), 7.49 (1H, d, Tp), 6.48 (1H, t, Tp), 6.29 (1H, t, Tp), 6.20 (1H, t, Tp), 4.30 (1H, m, aldehyde), 2.28 (3H, dd ( $J = 4.4, 1.0$ ), Me), 1.36 (9H, d ( $J = 8.7$ ), PMe<sub>3</sub>). <sup>13</sup>C NMR (acetone-*d*<sub>6</sub>,  $\delta$ ): 144.5 (s, Tp), 143.7 (s, Tp), 141.5 (s, Tp), 137.5 (s, Tp), 136.7 (s, Tp), 135.8 (s, Tp), 107.5 (s, Tp), 106.4 (s, Tp), 106.3 (s, Tp), 85.2 (d ( $J = 16.8$ ), bound (aldehyde)), 24.3 (s, Me), 13.3 (d ( $J = 30.5$ ), PMe<sub>3</sub>). Secondary diastereomer (**1A**): <sup>1</sup>H NMR (acetone-*d*<sub>6</sub>,  $\delta$ ): 8.22 (1H, d, Tp), 8.12 (1H, d, Tp), 7.97 (1H, d, Tp), 7.84 (1H, d, Tp), 7.77 (1H, d, Tp), 7.63 (1H, d, Tp), 6.42 (1H, t, Tp), 6.27 (1H, t, Tp), 6.21 (1H, t, Tp), 2.84 (1H, m, aldehyde), 2.32 (3H, d ( $J = 4.6$ ), Me), 1.35 (9H, d ( $J = 9.1$ ), PMe<sub>3</sub>). <sup>13</sup>C NMR (acetone-*d*<sub>6</sub>,  $\delta$ ) (CHO not reported): 145.4 (s, Tp), 143.2 (s, Tp), 142.6 (s, Tp), 137.2 (s, Tp), 137.1 (s, Tp), 136.0 (s, Tp), 107.1 (s, Tp), 106.5 (s, Tp), 106.3 (s, Tp), 23.3 (s, Me), 11.6 (d ( $J = 26$ ), PMe<sub>3</sub>). Monitoring by <sup>1</sup>H NMR of a sealed tube containing the initial crude mixture dissolved in acetone-*d*<sub>6</sub> gave the following results: The ratio of isomers was determined by relative integration of the resonances assigned to the methyl and aldehyde protons of the bound acetaldehyde for each isomer. Initially the ratio was 2:5:1 **1A**:**1B**:**1C**. After 2 days at ambient temperature, the ratio was 8:20:1. The tube was then heated for 4 days at 70 °C, and the ratio was then 20:40:1 (**1C** not visible). Further heating for 1 week at 70 °C did not change this ratio, nor was **4** observed.

**TpW(NO)(PMe<sub>3</sub>)( $\eta^2$ -acetone) (2).** TpW(NO)(PMe<sub>3</sub>)( $\eta^2$ -benzene) (557.8 mg, 0.960 mmol) was dissolved in reagent grade acetone and sat overnight. Orange crystals formed on the bottom of the reaction vessel were collected on a medium-porosity frit, washed with pentane, and dried in vacuo to give **2B** (173.0 mg, 0.3054 mmol, 32% yield). IR (HATR glaze):  $\nu_{\text{NO}} = 1546 \text{ cm}^{-1}$ . CV (DMA, TBAH, 100 mV/s, vs NHE):  $E_{\text{p,a}} = +0.46 \text{ V}, +0.71 \text{ V}$ . FAB-MS:  $m/z = 561 [\text{M}]^+$ . <sup>1</sup>H NMR (acetone-*d*<sub>6</sub>,  $\delta$ ): 8.25 (1H, d, Tp), 8.14 (1H, d, Tp), 7.97 (1H, d, Tp), 7.90 (1H, d, Tp), 7.83 (1H, d, Tp), 7.73 (1H, d, Tp), 6.42 (1H, t, Tp), 6.33 (1H, t, Tp), 6.26 (1H, t, Tp), 2.22 (3H, d ( $J = 0.9$ ), Me), 2.11 (3H, d ( $J = 1.5$ ), Me), 1.42 (9H, d ( $J = 8.9$ ), PMe<sub>3</sub>). <sup>13</sup>C NMR (acetone-*d*<sub>6</sub>,  $\delta$ ): 143.1 (s, Tp), 142.9 (s, Tp), 142.3 (s, Tp), 136.2 (s, Tp), 135.9 (s, Tp), 134.8 (s, Tp), 106.5 (s, Tp), 106.2 (s, Tp), 105.3 (s, Tp), 89.9 (d ( $J = 15.9$ ), CO), 33.0 (s, Me), 30.1 (s, Me), 14.7 (d ( $J = 28.1$ ), PMe<sub>3</sub>). <sup>31</sup>P NMR: (CDCl<sub>3</sub>,  $\delta$ ): -9.47 (satellite d ( $J = 295.6$ ), PMe<sub>3</sub>). Anal. Calcd for C<sub>15</sub>H<sub>25</sub>BN<sub>7</sub>O<sub>2</sub>PW: C, 34.92; H, 5.05; N, 15.84. Found: C, 35.11; H, 5.15; N, 15.29.

**Preparation of Product 2A.** Crystals of **2B** (27.2 mg) were dissolved in THF (2 mL) and refluxed overnight in a pressure tube (90 °C). The reaction solution was then added to pentane and the precipitate collected on a medium-porosity frit, washed with pentane (50 mL), and dried in vacuo to give **2A** (8.1 mg, 30% recovery) as a white powder. CV (DMA, TBAH, 100 mV/s, vs NHE):  $E_{\text{p,a}} = +0.44 \text{ V}, +0.71 \text{ V}$ . <sup>1</sup>H NMR (acetone-*d*<sub>6</sub>,  $\delta$ ): 8.18 (1H, d, Tp), 8.09 (1H, d, Tp), 7.93 (1H, d, Tp), 7.85 (1H, d, Tp), 7.80 (1H, d, Tp), 7.73 (1H, d, Tp), 6.39 (1H, t, Tp), 6.31 (1H, t, Tp), 6.23 (1H, t, Tp), 2.18 (3H, s, Me), 1.35 (9H, d ( $J = 9.2$ ), PMe<sub>3</sub>), 1.08 (3H, s, Me).

**TpW(NO)(PMe<sub>3</sub>)( $\eta^2$ -methyl formate) (3).** TpW(NO)(PMe<sub>3</sub>)-( $\eta^2$ -benzene) (617.9 mg, 1.063 mmol) was dissolved in 5 mL of methyl formate and stirred for 5 h. Next, the solvent was removed under reduced pressure and the residue was dissolved in CH<sub>2</sub>Cl<sub>2</sub>. The solution was then chromatographed on alumina (2 cm), first using CH<sub>2</sub>Cl<sub>2</sub> as the eluent. A pale pink fraction was collected and set aside (see **4**). Next the alumina was eluted with THF, a light brown fraction was collected, solvent was reduced to 10 mL, and 75 mL of pentane was added. The resulting precipitate was collected on a medium-porosity frit and dried in vacuo to give 24.6 mg of a tan powder (1:2:1 mixture of **3A**:**3B**:**3C** contaminated with **3H**). Attempts to further purify **3** by chromatography led to additional contamination by **3H**. IR (HATR glaze):  $\nu_{\text{NO}} = 1554 \text{ cm}^{-1}$ . <sup>1</sup>H NMR (acetone-*d*<sub>6</sub>,  $\delta$ ) (**3B** only): 8.16 (1H, d, Tp), 8.14 (1H, d, Tp), 8.02 (1H, d, Tp), 7.85 (1H, d, Tp), 7.81 (1H, d, Tp), 7.53 (1H, d, Tp), 6.69 (1H, d ( $J = 11.8$ ), formyl), 6.47 (1H, t, Tp), 6.33 (1H, t, Tp), 6.23 (1H, t, Tp), 3.40 (3H, s, OMe), 1.44 (9H, d ( $J = 9.2$ ), PMe<sub>3</sub>). <sup>13</sup>C NMR (CDCl<sub>3</sub>,  $\delta$ ) (**3B**): 146.3 (s, Tp), 143.7 (s, Tp), 143.1 (s, Tp), 142.3 (s, Tp), 137.5 (s, Tp), 135.9 (s, Tp), 117.3 (d ( $J = 21.1$ ), CHO), 106.6 (s, Tp), 106.5 (s, Tp), 106.1 (s, Tp), 53.16 (s, MeO), 13.3 (d ( $J = 30.2$ ), PMe<sub>3</sub> B). <sup>31</sup>P NMR: (acetone-*d*<sub>6</sub>,  $\delta$ ): (**3B**) -6.78 (satellite d ( $J = 307.0$ ), PMe<sub>3</sub>).

**TpW(NO)(PMe<sub>3</sub>)(H)(formate) (3H).** Further chromatography (on SiO<sub>2</sub>) of the impure product in **3** (vide supra) led to the production of more **3H** (**3H** eluted with 4:1 CH<sub>2</sub>Cl<sub>2</sub>/THF), which could also be prepared directly by dissolving TpW(NO)- (PMe<sub>3</sub>)( $\eta^2$ -benzene) (107 mg, 0.184 mmol) in DME (1 mL) and adding formic acid (~100 mg). After 2.5 h the reaction mixture was added to pentane (500 mL) and the resulting precipitate collected on a medium-porosity frit and dried in vacuo to give **3H** (64.7 mg, 0.118 mmol, 64%) as a yellow-green powder. IR (HATR glaze):  $\nu_{\text{NO}} = 1592 \text{ cm}^{-1}, \nu_{\text{CO}} = 1627 \text{ cm}^{-1}, \nu_{\text{WH}} = 1867 \text{ cm}^{-1}$  (w)  $\nu_{\text{BH}} = 2514 \text{ cm}^{-1}$ . CV (DMA, TBAH, 100 mV/s, vs NHE):  $E_{\text{p,a}} = +1.01 \text{ V}$ . FAB-MS:  $m/z = 548 [\text{M} - \text{H}]^+$ . <sup>1</sup>H NMR (acetone-*d*<sub>6</sub>,  $\delta$ ): 12.67 (1H, d ( $J = 128.2$ ), satellite dd ( $J = 128.2, 15.5$ ), W-H), 8.60 (1H, s, W-CO<sub>2</sub>H), 8.11 (1H, d, Tp), 8.06 (1H, d, Tp), 8.02 (1H, d, Tp), 7.99 (1H, d, Tp), 7.97 (1H, d, Tp), 7.73 (1H, d, Tp), 6.49 (1H, t, Tp), 6.33 (1H, t, Tp), 6.24 (1H, t, Tp), 1.44 (9H, d ( $J = 10.1$ ), PMe<sub>3</sub>). <sup>13</sup>C NMR (CDCl<sub>3</sub>,  $\delta$ ): 167.7 (s, CHO), 145.3 (s, Tp), 144.5 (s, Tp), 142.6 (s, Tp), 138.1 (s, Tp), 136.3 (s, Tp), 134.3 (s, Tp), 107.2 (s, Tp), 106.0 (s, Tp), 105.4 (s, Tp), 17.0 (d ( $J = 36.6$ ), PMe<sub>3</sub>). <sup>31</sup>P NMR (CDCl<sub>3</sub>,  $\delta$ ): 8.62 (satellite d ( $J = 144.6$ ), PMe<sub>3</sub>). Anal. Calcd for C<sub>13</sub>H<sub>21</sub>BN<sub>7</sub>O<sub>3</sub>PW: C, 28.44; H, 3.86; N, 17.86. Found: C, 28.35; H, 3.52; N, 17.39.

**TpW(NO)(PMe<sub>3</sub>)(CO) (4).** The pink fraction from the chromatography of **3** was stripped to 10 mL and added to 75 mL of pentane. The resulting precipitate was collected on a medium-porosity frit and dried in vacuo to give **4** (35.6 mg) as a pink powder. IR (HATR glaze):  $\nu_{\text{NO}} = 1580 \text{ cm}^{-1}, \nu_{\text{CO}} = 1864 \text{ cm}^{-1}$ . CV (DMA, TBAH, 100 mV/s, vs NHE):  $E_{1/2} = +0.32 \text{ V}$ . ESI<sup>+</sup>-MS:  $m/z = 532 [\text{M}]^+$ . <sup>1</sup>H NMR (acetone-*d*<sub>6</sub>,  $\delta$ ): 7.93 (2H, d, 2 Tp), 7.86 (1H, d, Tp), 7.84 (1H, d, Tp), 7.79 (1H, d, Tp), 7.77 (1H, d, Tp), 6.36 (1H, t, Tp), 6.26 (2H, t, 2 Tp), 1.56 (9H, d ( $J = 8.0$ ), PMe<sub>3</sub>). <sup>13</sup>C NMR (acetone-*d*<sub>6</sub>,  $\delta$ ): 251.1 (s, CO), 145.3 (s, Tp), 144.2 (s, Tp), 144.0 (s, Tp), 137.0 (s, Tp), 136.6 (s, Tp), 135.9 (s, Tp), 106.8 (s, Tp), 106.5 (s, 2 Tp), 17.5 (d ( $J = 30.5$ ), PMe<sub>3</sub>). <sup>31</sup>P NMR (acetone-*d*<sub>6</sub>,  $\delta$ ): -12.99 (satellite d ( $J = 372.4$ ), PMe<sub>3</sub>). Anal. Calcd for C<sub>13</sub>H<sub>19</sub>BN<sub>7</sub>O<sub>2</sub>PW: C, 29.41; H, 3.61; N, 18.47. Found: C, 30.01; H, 3.34; N, 18.19.

**TpW(NO)(PMe<sub>3</sub>)( $\eta^2$ -ethyl acetate) (5).** TpW(NO)(PMe<sub>3</sub>)-( $\eta^2$ -benzene) (87.0 mg, 0.149 mmol) was dissolved in EtOAc (1 mL). Pentane (3 mL) was added immediately and the resulting suspension was stirred overnight. More pentane (50 mL) was added to the reaction mixture, and the precipitate was collected on a medium-porosity frit and dried in vacuo to give **5** (23.9 mg) as a peach powder (contaminated with **5H**). Attempts to chromatograph **5** led to the production of increased quantities of **5H**. IR (HATR glaze):  $\nu_{\text{NO}} = 1552 \text{ cm}^{-1}$ . <sup>1</sup>H NMR (acetone-*d*<sub>6</sub>,  $\delta$ ) (**5A** and **5B**): 8.22 (1H, d, Tp), 8.16 (1H, d, Tp),



8.12 (2H, d, Tp), 8.05 (1H, d, Tp), 8.01 (1H, d, Tp), 7.94 (1H, d, Tp), 7.87 (1H, d, Tp), 7.85 (1H, d, Tp), 7.83 (1H, d, Tp), 7.81 (1H, d, Tp), 7.59 (1H, d, Tp), 6.45 (1H, t, Tp), 6.39 (1H, t, Tp), 6.32 (1H, t, Tp), 6.30 (1H, t, Tp), 6.24 (1H, t, Tp), 6.20 (1H, t, Tp), 3.84 (1H, m, CH<sub>2</sub>), 3.70 (1H, m, CH<sub>2</sub>), 3.62 (1H, m, CH<sub>2</sub>), 3.51 (1H, m, CH<sub>2</sub>), 2.36 (3H, s, acetyl Me (**5B**)), 1.43 (9H, d ( $J = 9.0$ ), PMe<sub>3</sub>), 1.38 (9H, d ( $J = 9.3$ ), PMe<sub>3</sub>), 1.17 (3H, t ( $J = 7.2$ ), OCH<sub>2</sub>CH<sub>3</sub>), 1.14 (3H, t ( $J = 7.2$ ), OCH<sub>2</sub>CH<sub>3</sub>), 1.01 (3H, s, acetyl Me (**5A**)). <sup>13</sup>C NMR (acetone-*d*<sub>6</sub>,  $\delta$ ): 144.8 (s, Tp), 144.4 (s, Tp), 144.1 (s, Tp), 143.7 (s, Tp), 143.5 (s, Tp), 143.3 (s, Tp), 137.3 (s, Tp), 137.0 (s, Tp), 136.9 (s, Tp), 136.8 (s, Tp), 136.0 (s, Tp), 135.8 (s, Tp), 119.6 (d ( $J = 22.0$ ), CO (**5B**)), 116.7 (d ( $J = 3.7$ ), CO (**5A**)), 107.4 (s, Tp), 107.0 (s, Tp), 106.4 (s, 2 Tp), 106.2 (s, Tp), 105.6 (s, Tp), 61.2 (s, CH<sub>2</sub>), 56.3 (s, CH<sub>2</sub>), 27.1 (s, acetyl (**5A**)), 26.1 (d ( $J = 2.7$ ), acetyl (**5B**)), 16.7 (s, OCH<sub>2</sub>CH<sub>3</sub>), 16.5 (s, OCH<sub>2</sub>CH<sub>3</sub>), 14.5 (d ( $J = 29.3$ ), PMe<sub>3</sub>), 11.4 (d ( $J = 27.5$ ), PMe<sub>3</sub>). <sup>31</sup>P NMR: (acetone-*d*<sub>6</sub>,  $\delta$ ): -6.99 (satellite d ( $J = 308.4$ ), PMe<sub>3</sub>), -9.41 (satellite d ( $J = 296.0$ ), PMe<sub>3</sub>).

**TpW(NO)(PMe<sub>3</sub>)(H)(acetate) (5H).** TpW(NO)(PMe<sub>3</sub>)( $\eta^2$ -benzene) (666.6 mg, 1.147 mmol) was dissolved in DME (7 mL), and then acetic acid was added and the reaction sat for 3 h. The solvent was then removed under reduced pressure and redissolved in 1.5 mL of DME. The solution was then chromatographed on silica (2 cm) using 1:1 Et<sub>2</sub>O/THF as the eluent. A light brown fraction was collected and the solvent reduced to 3 mL. Pentane (75 mL) was added, and the resulting precipitate was collected on a medium-porosity frit and dried in vacuo to give **5H** (308.6 mg, 0.548 mmol, 48% yield) as a pale yellow powder. **5H** was also obtained from attempts to chromatograph crude **5** on SiO<sub>2</sub> (**5H** was eluted with THF). IR (HATR glaze):  $\nu_{\text{NO}} = 1585 \text{ cm}^{-1}$ ,  $\nu_{\text{CO}} = 1632 \text{ cm}^{-1}$ ,  $\nu_{\text{WH}} = 1891 \text{ cm}^{-1}$ ,  $\nu_{\text{BH}} = 2490 \text{ cm}^{-1}$ . CV (DMA, TBAH, 100 mV/s, vs NHE):  $E_{\text{p,a}} = +0.94 \text{ V}$ . FAB-MS:  $m/z = 562 [\text{M} - \text{H}]^+$ . <sup>1</sup>H NMR (acetone-*d*<sub>6</sub>,  $\delta$ ): 13.22 (1H, d ( $J = 130.3$ ), sat. dd ( $J = 130.3, 13.1$ ), W-H), 8.13 (1H, d, Tp), 8.09 (1H, br s, Tp), 8.05 (2H, bs s, 2 Tp), 7.94 (1H, d, Tp), 7.73 (1H, d, Tp), 6.48 (1H, t, Tp), 6.28 (1H, t, Tp), 6.24 (1H, t, Tp), 1.81 (3H, s, CH<sub>3</sub>), 1.41 (9H, d ( $J = 10.1$ ), PMe<sub>3</sub>). <sup>13</sup>C NMR (acetone-*d*<sub>6</sub>,  $\delta$ ): 173.32 (s, CO), 146.7 (s, Tp), 145.3 (s, Tp), 142.7 (s, Tp), 139.0 (s, Tp), 137.3 (s, Tp), 135.5 (s, Tp), 108.0 (s, Tp), 106.3 (s, Tp), 106.0 (s, Tp), 24.2 (s, CH<sub>3</sub>), 16.7 (d ( $J = 35.1$ ), PMe<sub>3</sub>). <sup>31</sup>P NMR (acetone-*d*<sub>6</sub>,  $\delta$ ): 9.02 (satellite d ( $J = 150.8$ ), PMe<sub>3</sub>). Anal. Calcd for C<sub>14</sub>H<sub>23</sub>WPO<sub>3</sub>N<sub>7</sub>B: C, 29.87; H, 4.12; N, 17.42. Found: C, 30.14; H, 4.04; N, 17.87.

**Decarbonylation of DMF by {TpW(NO)(PMe<sub>3</sub>)} to Give **4**.** TpW(NO)(PMe<sub>3</sub>)( $\eta^2$ -benzene) (97.0 mg, 0.1669 mmol) was dissolved in neat DMF. The mixture sat for 1 h and was subsequently heated in a sealed tube to 90 °C for 4 h. Monitoring by IR indicated the presence of **4** ( $\nu_{\text{CO}} = 1864 \text{ cm}^{-1}$  and  $\nu_{\text{NO}} = 1580 \text{ cm}^{-1}$ ), the CO complex. The product was isolated by column chromatography on silica (as above) in 5% yield (4.0 mg, 0.0075 mmol) as a pale pink powder. <sup>1</sup>H NMR confirmed the product's identity. The dissolution of **6** in neat DMF followed by heating yielded similar results.

**Decarbonylation of DMF by {TpRe(CO)(MeIm)} to Give TpRe(CO)<sub>2</sub>(MeIm).** TpRe(CO)(MeIm)( $\eta^2$ -benzene)<sup>28</sup> (50.1 mg, 0.0853 mmol) was dissolved in DME to which was added DMF (1 mL). After 24 h, the solvent of the reaction mixture was removed under reduced pressure. The residue was redissolved in DME and added to pentane (50 mL) to form a white precipitate, which was collected on a medium-porosity frit and dried in vacuo to give TpRe(CO)<sub>2</sub>(MeIm)<sup>42</sup> (28.0 mg, 0.0521 mmol) as a white powder in 61% yield. <sup>1</sup>H NMR and IR confirmed the product's identity.

**TpMo(NO)(MeIm)(CO) (8).** This compound was previously reported.<sup>19</sup> Additional data: <sup>13</sup>C NMR (acetone-*d*<sub>6</sub>,  $\delta$ ): 230.9 (s, CO). CV (DMA, TBAH, 100 mV/s, vs NHE):  $E_{1/2} = +0.08 \text{ V}$ .

**TpMo(NO)(MeIm)( $\eta^2$ -acetone) (9).** (Alternate synthesis). A THF solution of TpMo(NO)(MeIm)Br was stirred overnight

with 20 equiv of acetone and 1% Na/Hg. The resulting reaction mixture was isolated by chromatography on silica by elution with a 1:3 THF/diethyl ether, followed by precipitation into pentane to form a green powder in 67% yield.

**TpMo(NO)(MeIm)( $\eta^2$ -*N,N*-dimethylformamide) (10).** To a THF solution (125 mL) of TpMo(NO)(MeIm)Br (388 mg, 774  $\mu\text{mol}$ ) and DMF (13.1 g, 0.0179 mol) was added 1.03% sodium/mercury amalgam (7.3 g), and the mixture was stirred for 24 h. The solution was decanted away from the mercury amalgam, and the solvent was removed under reduced pressure. The residue was dissolved in a minimal amount of THF and was subjected to flash chromatography, eluting first with diethyl ether, next with 1:3 THF/diethyl ether, and finally with neat THF (product elution) to afford a greenish-yellow eluent. The solvent was removed under reduced pressure to 10 mL, and pentane (100 mL) was added to afford a beige precipitate. The solid was collected and dried in vacuo. Typical yields: 30–35%. CV (DMA, TBAH, 100 mV/s, vs NHE):  $E_{\text{p,c}} = -1.13 \text{ V}$ ,  $E_{\text{p,a}} = -0.70 \text{ V}$ ,  $+0.85 \text{ V}$ . IR (HATR, glaze):  $\nu_{\text{NO}} = 1558 \text{ cm}^{-1}$ . <sup>1</sup>H NMR (500 MHz) (acetone-*d*<sub>6</sub>,  $\delta$ , -90 °C): 8.16, 7.95, 7.87, 7.80, 7.69, 7.11 (1H each, each a br s, Tp), 6.26 (2H, s, Tp), 6.12 (1H, s, Tp), 7.11, 6.68 (1H each, each a t (Im)), 7.37 (1H, d, (Im)), 3.86 (3H, s, (N-Me)), 4.97 (1H, s, formyl H), 2.64 (6H, s, N-Me). Anal. Calcd for C<sub>16</sub>H<sub>23</sub>MoO<sub>2</sub>N<sub>10</sub>B: 38.89; H, 4.69; N, 28.34. Found: C, 38.49; H, 4.65; N, 28.71.

## Conclusion

The three heavy metal  $\pi$  bases {TpW(NO)(PMe<sub>3</sub>)}, {TpRe(NO)(MeIm)}, and {Os(NH<sub>3</sub>)<sub>5</sub>}<sup>2+</sup> have similar d<sup>5</sup>/d<sup>6</sup> reduction potentials,<sup>50</sup> inner sphere coordination geometries, and abilities to form stable  $\eta^2$ -coordinate complexes with benzenes. Yet, their abilities to form analogous complexes with carboxylic acid derivatives vary considerably. Whereas osmium can only bind aldehydes and ketones across the carbonyl group, the rhenium system is capable of forming  $\eta^2$ -ester complexes as well, and the tungsten system forms an  $\eta^2$ -DMF complex that resists decarbonylation and substitution under ambient conditions. The molybdenum analogue {TpMo(NO)(MeIm)}, while unable to form a stable complex with benzene, has a reduction potential similar to that of its congener and also binds DMF across the carbonyl, giving rise to the first example of a second-row transition metal to form a  $\pi$  complex with a carboxylic acid derivative. These osmium and rhenium systems react with DMF at 20 °C to give the CO complex. However, the  $\eta^2$ -DMF complexes of the group 6 metals fail to decarbonylate at this temperature, owing to the stability of the  $\eta^2$ -binding mode for these metals.

**Acknowledgment** is made to the donors of the Petroleum Research Fund, administered by the ACS, for partial support of this research (ACS-PRF#36638-AC1). This work was also supported by the NSF (CHE0111558 and 9974875) and the NIH (NIGMS: R01-GM49236).

**Supporting Information Available:** This material is available free of charge via the Internet at <http://pubs.acs.org>. OM049016E

(50) The reduction potentials corresponding to analogous arene or alkene complexes are within 300 mV.